



Short communication

Design and synthesis of novel 5-phenyl-*N*-piperidine ethanone containing 4,5-dihydropyrazole derivatives as potential antitumor agentsXin-Hua Liu ^{a,b,*}, Jun Li ^a, Jing Bo Shi ^a, Bao-An Song ^{b,**}, Xing-Bao Qi ^c^a School of Pharmacy, Anhui Medical University, Hefei 230032, PR China^b Key Laboratory of Green Pesticide and Agricultural Bioengineering, Ministry of Education, Guizhou University, Guiyang 550025, PR China^c School of Pharmacy, China Pharmaceutical University, Nanjing 210009, PR China

ARTICLE INFO

Article history:

Received 8 February 2012

Received in revised form

17 February 2012

Accepted 18 February 2012

Available online 25 February 2012

Keywords:

Synthesis

Piperidine

4,5-Dihydropyrazole

Antitumor agents

ABSTRACT

A series of novel 5-phenyl-*N*-piperidine ethanone-4,5-dihydropyrazole derivatives as potential telomerase inhibitors were synthesized. The bioassays demonstrated that compounds **4d**, **4f**, **7a** and **7b** occupied high antiproliferative activities against SGC-7901, MGC-803 and Bcap-37 cell lines. By a modified TRAP assay, some titled compounds were tested against telomerase, and compound **7b** showed the most potent inhibitory activity with IC₅₀ value at 2.00 ± 0.40 μM. The active compound **4d** was also docked into the telomerase TERT active site to determine the probable binding model. The results indicated that conserved residues Lys189, Asp254 and Gln308 were important for ligand binding via hydrogen bond interactions.

© 2012 Elsevier Masson SAS. All rights reserved.

1. Introduction

Telomerase remains active in the early stages of life maintaining telomere length and the chromosomal integrity of frequently dividing cells. It turns dormant in most somatic cells during adulthood [1]. In cancer cells, however, telomerase gets reactivated and works tirelessly to maintain the short length of telomeres of rapidly dividing cells, leading to their immortality [2]. The essential role of telomerase in cancer and ageing makes it an important target for the development of therapies to treat cancer and other age-associated disorders. Telomere and telomerase are closely related to the occurrence and development of human gastric cancer [3].

Dihydropyrazole, a small bioactive molecule, is a prominent structural motif found in numerous pharmaceutically active compounds [4,5]. The dihydropyrazole structure has been demonstrated to bear important biological activities such as anticancer, antimicrobial, antimalarial, antinociceptive, antiviral, anti-tubercular, anti-inflammatory [6–8].

In our recent publications [9,10], several dihydropyrazole derivatives were described, which had potent anticancer activity, especially against SGC-7901 cell line. According to preliminary anticancer activity of structure–activity relationship (SAR), we found that anticancer activity changed with the transformation of *N*-acetyl. The novel docking model based on the protein structure of telomerase inhibitors was developed using LigandFit module within Discovery Studio 2.1, we found 4,5-dihydropyrazole ring project into a hydrophobic region, which was comprised of the side chains of 220–260, that was important for the potent inhibitory activity [9]. In current molecular design, when the hydrogen atom of *N*-acetyl was replaced by piperidine, the 5-phenyl 4,5-dihydropyrazole ring projected into a more stable hydrophobic region, which comprised of the side chains of 252–256, should be enhance the anticancer activity. So we designed and synthesized some 5-phenyl-dihydropyrazole derivatives containing piperidine moiety.

Furthermore, tetracyclic coumarin compounds, have been demonstrated to bear the best anti-HIV-1 virus activity. Because of the mechanistic and structural similarity between reverse transcriptases and hTERT, it is supposed that known reverse transcriptase inhibitors may potently inhibit human telomerase [11,12]. Based on this hypothesis, since there are only a very few systematic reports on the synthetic methodology and evaluation of anticancer activities of these compounds, we introduced the coumarin

* Corresponding author. School of Pharmacy, Anhui Medical University, Hefei, 230032, PR China. Tel./fax: +86 551 5161115.

** Corresponding author. Tel.: +86 851 3620521; fax: +86 851 3622211.

E-mail addresses: xhliuhx@163.com (X.-H. Liu), songbaoan22@yahoo.com (B.-A. Song).

moiety in the above-mentioned 5-phenyl-dihydropyrazole piperidine skeleton, designed and synthesized of *N*-substituted-dihydropyrazole-piperidine derivatives containing coumarin moiety.

In order further investigate the detailed structural basis of the synthesized inhibitor for telomerase TERT, high inhibitory activity compound was docked into the active site of telomerase TERT (3DU6).

2. Results and discussion

2.1. Chemistry

The synthesis of compound **5** (Scheme 2) started from salicylaldehyde and catalyzed by piperazine at 20–30 °C was added acetoacetate. Claisen–Schmidt condensation 3-acetyl-2*H*-chromen-2-one and benzaldehyde using mild catalyst piperazine, by following a reported method [10], proved to be an efficient method for the synthesis of α,β unsaturated ketone **5**. Using catalysts DMAP, proved to be an efficient alternative method for the synthesis of title compounds **4**, **7**. In addition, in order to facilitate the synthesis of target compound **4**, catalytic amount of KI was added. In the process of synthesis of compound **7**, the best choice to control pH value less than 8.5 with organic base, when the pH value is greater than 8.5, the coumarin ring will open. Compounds **1–3** were prepared according to a previously published report [13].

In order to facilitate molecular docking, the structures of compounds **4d** and **7b** were determined by X-ray crystallography. Crystal data of **4d**: Colorless crystals, yield, 64%; mp 159 °C; C₁₈H₂₅N₃O₂, *M* = 315.4, Orthorhombic, space group *P*2₁2₁2₁; *a* = 7.571(5), *b* = 11.028(8), *c* = 21.407(15) (Å); α = 90, β = 90, γ = 90(°), *V* = 1787(2) nm³, *T* = 293(2) K, *Z* = 4, *D*_c = 1.172 g/cm³, *F*(000) = 680, Reflections collected/unique = 7851/2989, Data/restraints/parameters = 2989/3/208, Goodness of fit on *F*² = 1.027, Fine, *R*₁ = 0.0258, *wR*(*F*²) = 0.2970. Crystal data of **7b**: colorless crystals, yield, 59%; mp 209–211 °C; C₂₆H₂₉N₃O₄, *M* = 447.5, Triclinic, space group *P*-1; *a* = 9.425(4), *b* = 10.453(4), *c* = 13.384(6) (Å); α = 103.385(4), β = 103.263(4), γ = 95.469(4) (°), *V* = 1233.1(9) nm³, *T* = 293(2) K, *Z* = 2, *D*_c = 1.205 g/cm³, *F*(000) = 476, Reflections collected/unique = 9122/4688, Data/restraints/parameters = 4688/0/298, Goodness of fit on *F*² = 1.003, Fine, *R*₁ = 0.078, *wR*(*F*²) = 0.2050.

The molecular structures of compounds **4d** and **7b** were shown in Figs. 1 and 2. Crystallographic data (excluding structure factors) for the structure had been deposited with the Cambridge

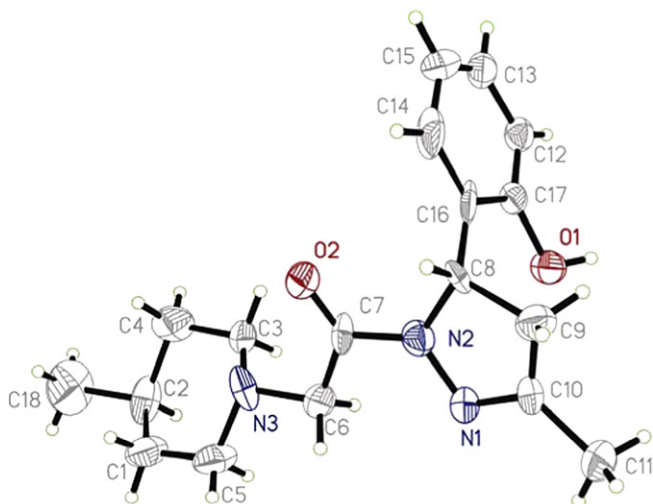


Fig. 1. ORTEP drawing of compound **4d**.

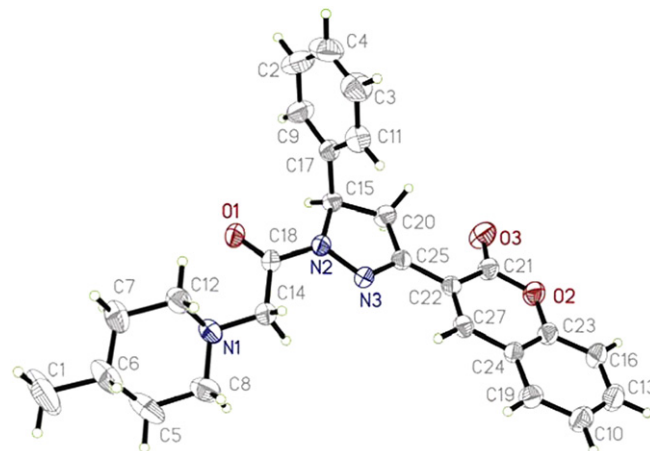


Fig. 2. ORTEP drawing of compound **7b**.

Crystallographic Data Center as supplementary publication No. CCDC-837387 and CCDC-836554. These data can be obtained free of charge via the URL <http://www.ccdc.cam.ac.uk/conts/retrieving.html> (or from the CCDC, 12 Union Road, Cambridge CB2 1EZ, UK; fax: (+44) 1223 336033; e-mail: deposit@ccdc.cam.ac.uk).

2.2. In vitro anticancer activity

In the screening assay studies, all title compounds were evaluated for their cytotoxic activity against gastric SGC-7901, MGC-803 and Bcap-37 cell lines. Also included were the activities of reference compound 5-fluorouracil. The cell was allowed to proliferate in presence of tested material for 48 h, and the results are reported in terms of IC₅₀ values (Table 1). It is obvious from the data that compounds **4f**, **7b** exhibited high activity against SGC-7901 and MGC-803 with the IC₅₀ values of 3.22 ± 0.40, 2.64 ± 0.31 and 4.70 ± 0.09, 3.01 ± 0.24 μM respectively, surpassing that of the positive control 5-fluorouracil. Compounds **7a**, **7b** showed anticancer activity against the Bcap-37 with IC₅₀ values of 7.30 ± 1.01, 6.57 ± 0.34 μM respectively, comparable to that of positive control 5-fluorouracil. From the data presented in Table 1, it can be concluded that *N*-substituted-dihydropyrazole-piperidine-coumarin derivatives, in general, showed relatively higher activity against SGC-7901, MGC-803 and Bcap-37 cell lines (**7a–c**), so, some compounds in this series deserve further investigation.

Table 1

Cytotoxic activity of the synthesized compounds against SGC-7901, MGC-803 and Bcap-37 cell lines.^a

Compound	IC ₅₀ (μM) ^b		
	SGC-7901	MGC-803	Bcap-37
4a	5.71 ± 0.78	4.12 ± 0.87	18.70 ± 2.47
4b	11.22 ± 1.31	11.70 ± 1.45	16.33 ± 2.55
4c	12.91 ± 0.28	15.74 ± 1.26	10.70 ± 1.40
4d	4.60 ± 0.30	3.55 ± 0.19	6.81 ± 0.87
4e	39.22 ± 1.51	38.79 ± 2.11	41.05 ± 2.74
4f	3.22 ± 0.40	2.64 ± 0.31	8.55 ± 2.01
4g	30.71 ± 2.20	28.27 ± 2.00	32.31 ± 2.66
7a	6.00 ± 0.51	8.71 ± 0.45	7.30 ± 1.01
7b	4.70 ± 0.09	3.01 ± 0.24	6.57 ± 0.34
7c	10.33 ± 0.89	7.01 ± 0.29	8.76 ± 0.44
5-Fluorouracil ^c	7.11 ± 0.33	3.42 ± 15	5.33 ± 0.27

Negative control DMSO, no activity.

^a The data represented the mean of three experiments in triplicate and were expressed as means ± SD; Only descriptive statistics were done in the text.

^b The IC₅₀ value was defined as the concentration at which 50% survival of cells was observed. The results are listed in the table.

^c Used as a positive control.

Some purified title compounds were assayed for telomerase inhibition, using a MGC-803 cell extract, also included the activity of reference compound ethidium bromide. The results were summarized in Table 2. The results suggested that the compound **7b** showed strong telomerase inhibitory ability with IC_{50} value of $2.00 \pm 0.40 \mu\text{M}$, which surpassing that of the positive control ethidium bromide.

2.3. Molecular docking

In an effort to elucidate the mechanism by which the title compound can induce anticancer activity against above cancer cell lines and to establish an SAR based on our experimental studies, molecular docking of the potent inhibitor **4d** into binding site of telomerase was performed to simulate a binding model derived from telomerase TERT (3DU6 pdb). The binding model of compounds **4d** with telomerase TERT was depicted in Fig. 3. Visual inspection of the pose of **4d** into the ATP-site revealed that three more optimal intramolecular hydrogen bonds were observed ($\text{N}-\text{H}\cdots\text{N}-$, with amino hydrogen group of Lys189; $\text{N}-\text{H}\cdots\text{O}-\text{H}$, with amino hydrogen group of Asp254, $\text{N}-\text{H}\cdots\text{O}-\text{C}$, with amino hydrogen group of Gln308). In the other end of the ATP-binding pocket, the N of peridine interacted with the residue Phe 193, which made the 3D structure more stable [10].

3. Conclusion

In summary, we designed 5-phenyl-4,5-dihydropyrazole containing piperidine ethanone derivatives as potential telomerase inhibitors, followed by chemical synthesis and biological evaluated for their antiproliferative activities against several cell lines including MGC-803, Bcap-37 and SGC-7901. Compounds **4d**, **4f**, **7a** and **7b** occupied high antiproliferative activities against above cell lines. Compound **7b** showed the most potent inhibitory activity with IC_{50} value at $2.00 \pm 0.40 \mu\text{M}$. In addition, the binding mode of high active compound **4d** on the telomerase TERT indicated that conserved residues Lys189, Asp254 and Gln308 are important for ligand binding via hydrogen bond interactions. These results are of help in the rational design of more efficient telomerase inhibitors for chemoprevention and chemotherapy in further.

4. Experimental

4.1. Chemistry

The reactions were monitored by thin layer chromatography (TLC) on Merck pre-coated silica GF254 plates. Melting points (uncorrected) were determined on a XT4MP apparatus (Taikang Corp., Beijing, China). ^1H NMR, ^{13}C NMR spectra were collected on PX400 spectrometer at room temperature with TMS and solvent signals allotted as internal standards. Chemical shifts are reported in ppm (δ). Elemental analyses were performed on a CHN-O-Rapid instrument, and were within $\pm 0.4\%$ of the theoretical values.

Table 2
Inhibitory effects of selected compounds against telomerase.

Compound	IC_{50} (μM) Telomerase ^a
4a	9.11 ± 0.77
4d	5.99 ± 0.31
4f	8.81 ± 0.25
4g	42.12 ± 1.87
7b	2.00 ± 0.40
7c	4.11 ± 0.55
Ethidium bromide ^b	2.47 ± 0.29

^a Telomerase supercoiling activity.

^b Ethidium bromide is reported as a control. The inhibition constant of ethidium toward telomerase has been reported previously.

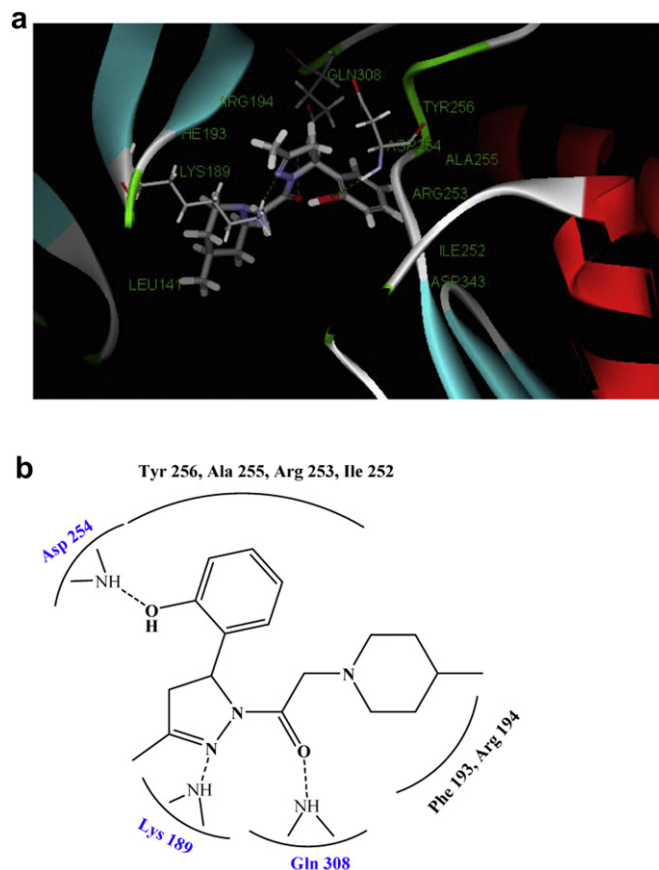


Fig. 3. Molecular docking modeling of compound **4d** (A) with telomerase TERT (3DU6); the small molecule and the critical interaction of 3DU6 are represented by sticks. (B) Schematic representation of the binding mode of **4d** in the ATP-binding site of 3DU6.

4.2. General procedure for the synthesis of compound **4**

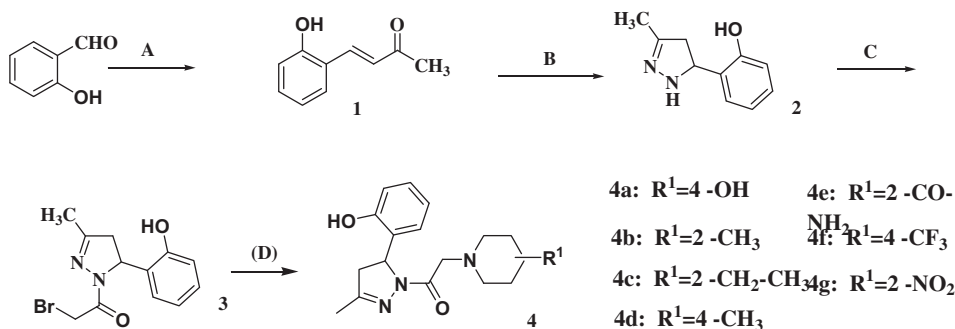
To an acetone (20 mL) solution of 2-bromo-1-(5-(2-hydroxyphenyl)-3-methyl-4,5-dihydropyrazol-1-yl)ethanone **3** (10 mmol) was added substituted-piperazine (10 mmol), DMAP (12 mmol) and catalytic KI, the reaction mixture was allowed to stand at $40-50^\circ\text{C}$ for 4 h. The mixture was cooled, washed with water. The product was collected by filtration and the crude residue was purified by chromatography on SiO_2 (dichloromethane/methanol, v:v = 65:1) to give title compounds **4a-g** (Scheme 1) as colorless solids.

4.2.1. 1-(5-(2-Hydroxyphenyl)-3-methyl-4,5-dihydropyrazol-1-yl)-2-(4-hydroxypiperidin-1-yl) ethanone (**4a**)

Colorless crystals, yield, 64%; mp $179-181^\circ\text{C}$; ^1H NMR (400 MHz, CDCl_3) δ (ppm): 1.60–1.67 (m, 2H), 1.83–1.91 (m, 2H), 2.18 (s, 3H), 2.31–2.37 (m, 2H), 2.83–2.86 (m, 2H), 3.05 (dd, 1H, $J_1 = 18.8$ Hz, $J_2 = 3.0$ Hz, pyrazole 4- H_a), 3.33 (dd, 1H, $J_1 = 18.4$ Hz, $J_2 = 11.2$ Hz, pyrazole 4- H_b), 3.52 (s, 2H), 3.66–3.70 (m, 1H), 5.65 (dd, 1H, $J_1 = 11.2$ Hz, $J_2 = 3.2$ Hz, pyrazole 5-H), 6.87–6.98 (m, 3H), 7.18–7.22 (m, 1H). Anal. calcd for $\text{C}_{17}\text{H}_{23}\text{N}_3\text{O}_3$: C, 64.33; H, 7.30; N, 13.24%. Found: C, 64.00; H, 7.66; N, 12.85%.

4.2.2. 1-(5-(2-Hydroxyphenyl)-3-methyl-4,5-dihydropyrazol-1-yl)-2-(2-methylpiperidin-1-yl) ethanone (**4b**)

Colorless crystals, yield, 60%; mp $190-191^\circ\text{C}$; ^1H NMR (400 MHz, CDCl_3) δ (ppm): 1.25 (d, 3H, $J = 6.0$ Hz), 1.46–1.48 (m, 1H), 1.71–1.77 (m, 4H), 1.88–1.96 (m, 1H), 2.12 (s, 3H), 2.92 (dd, 1H, $J_1 = 18.4$ Hz, $J_2 = 3.2$ Hz, pyrazole 4- H_a), 3.11–3.21 (m, 2H, containing pyrazole 4- H_b), 3.40 (s, 2H), 3.97–4.01 (m, 1H), 4.11–4.17



Scheme 1. Synthesis of title compound **4**. Reagent and conditions: (A) CH_3COCH_3 , $\text{C}_2\text{H}_5\text{ONa}$, 20–30 °C, 10 h. (B) $\text{NH}_2\text{-NH}_2\cdot\text{H}_2\text{O}$, $\text{C}_2\text{H}_5\text{OH}$, reflux, 3 h. (C) BrCH_2COOH , 40–50 °C, 2 h. (D) substituted piperidine DMAP, 60 °C, 4 h.

(m, 1H), 5.61 (dd, 1H, $J_1 = 11.2$ Hz, $J_2 = 3.2$ Hz, pyrazole 5-H), 6.82–6.86 (m, 1H), 6.90–6.93 (m, 1H), 7.02–7.04 (m, 1H), 7.11–7.15 (m, 1H). Anal. calcd for $\text{C}_{18}\text{H}_{25}\text{N}_3\text{O}_2$: C, 68.44; H, 7.99; N, 13.32%. Found: C, 68.71; H, 7.65; N, 12.97%.

4.2.3. 2-(2-Ethylpiperidin-1-yl)-1-(5-(2-hydroxyphenyl)-3-methyl-4,5-dihydropyrazol-1-yl)ethanone (**4c**)

Colorless crystals, yield, 52%; mp 166–167 °C; ^1H NMR (400 MHz, CDCl_3) δ (ppm): 0.89–0.97 (t, 3H, $J = 7.2$ Hz), 1.74–2.06 (m, 8H), 2.09 (s, 3H), 2.78 (dd, 1H, $J_1 = 18.4$ Hz, $J_2 = 3.4$ Hz, pyrazole 4- H_a), 3.35 (dd, 1H, $J_1 = 18.4$ Hz, $J_2 = 11.2$ Hz, pyrazole 4- H_b), 3.40–3.51 (m, 3H), 4.18–4.26 (m, 2H), 5.63 (dd, 1H, $J_1 = 11.2$ Hz, $J_2 = 3.4$ Hz, pyrazole 5-H), 6.78–6.92 (m, 2H), 7.01–7.10 (m, 1H), 7.17–7.19 (m, 1H). ^{13}C NMR (CDCl_3 , 125 MHz): δ 10.1, 16.3, 21.9, 22.2, 26.6, 27.4, 45.3, 56.0, 59.1, 64.8, 118.1, 120.8, 126.2, 126.7, 129.6, 153.8, 154.0, 160.9, 161.7; Anal. calcd for $\text{C}_{19}\text{H}_{27}\text{N}_3\text{O}_2$: C, 69.27; H, 8.26; N, 12.76%. Found: C, 69.00; H, 8.49; N, 13.04%.

4.2.4. 1-(5-(2-Hydroxyphenyl)-3-methyl-4,5-dihydropyrazol-1-yl)-2-(4-methylpiperidin-1-yl)ethanone (**4d**)

Colorless crystals, yield, 64%; mp 159–160 °C; ^1H NMR (400 MHz, CDCl_3) δ (ppm): 0.93–1.00 (d, 3H), 1.59–1.83 (m, 4H), 2.12 (s, 3H), 2.72–2.77 (m, 2H), 2.84 (dd, 1H, $J_1 = 18.4$ Hz, $J_2 = 3.3$ Hz, pyrazole 4- H_a), 2.90–2.97 (m, 1H), 3.28–3.37 (m, 2H), 3.41 (dd, 1H, $J_1 = 18.4$ Hz, $J_2 = 11.2$ Hz, pyrazole 4- H_b), 3.96 (s, 2H), 5.66 (dd, 1H, $J_1 = 11.2$ Hz, $J_2 = 3.3$ Hz, pyrazole 5-H), 6.83–6.95 (m, 2H), 7.07–7.15 (m, 2H). Anal. calcd for $\text{C}_{18}\text{H}_{25}\text{N}_3\text{O}_2$: C, 68.54; H, 7.99; N, 13.32%. Found: C, 68.81; H, 7.65; N, 13.55%.

4.2.5. 1-(2-(5-(2-Hydroxyphenyl)-3-methyl-4,5-dihydropyrazol-1-yl)-2-oxoethyl)piperidine-4-carboxamide (**4e**)

Colorless crystals, yield, 55%; mp 157–158 °C; ^1H NMR (400 MHz, CDCl_3) δ (ppm): 1.74–1.82 (m, 4H), 2.13 (s, 3H), 2.09–2.23 (m, 2H), 2.91 (dd, 1H, $J_1 = 18.8$ Hz, $J_2 = 3.2$ Hz, pyrazole 4- H_a), 2.97–3.02 (m, 2H), 3.31 (dd, 1H, $J_1 = 18.8$ Hz, $J_2 = 11.1$ Hz, pyrazole 4- H_b), 3.54 (s, 2H), 5.64 (dd, 1H, $J_1 = 11.2$ Hz, $J_2 = 3.2$ Hz, pyrazole 5-H), 5.92 (s, 2H), 6.82–6.90 (m, 4H), 7.10–7.14 (m, 1H). Anal. calcd for $\text{C}_{18}\text{H}_{24}\text{N}_4\text{O}_3$: C, 62.77; H, 7.02; N, 16.27%. Found: C, 62.43; H, 7.35; N, 16.12%.

4.2.6. 1-(5-(2-Hydroxyphenyl)-3-methyl-4,5-dihydropyrazol-1-yl)-2-(4-(trifluoromethyl)piperidin-1-yl)ethanone (**4f**)

Colorless crystals, yield, 66%; mp 170–172 °C; ^1H NMR (400 MHz, CDCl_3) δ (ppm): 1.68–1.86 (m, 4H), 2.07 (s, 3H), 2.48–2.79 (m, 5H), 2.99 (dd, 1H, $J_1 = 18.3$ Hz, $J_2 = 3.2$ Hz, pyrazole 4- H_a), 3.48 (dd, 1H, $J_1 = 18.3$ Hz, $J_2 = 11.2$ Hz, pyrazole 4- H_b), 3.61 (s, 2H), 5.75 (dd, 1H, $J_1 = 11.2$ Hz, $J_2 = 3.2$ Hz, pyrazole 5-H), 6.87–6.92 (m, 2H), 7.02–7.11 (m, 2H). Anal. calcd for $\text{C}_{18}\text{H}_{22}\text{F}_3\text{N}_3\text{O}_2$: C, 58.53; H, 6.00; N, 11.38%. Found: C, 58.51; H, 6.37; N, 10.99%.

4.2.7. 1-(5-(2-Hydroxyphenyl)-3-methyl-4,5-dihydropyrazol-1-yl)-2-(2-nitropiperidin-1-yl)ethanone (**4g**)

Colorless crystals, yield, 67%; mp 194–195 °C; ^1H NMR (400 MHz, CDCl_3) δ (ppm): 1.66–1.78 (m, 4H), 2.10 (s, 3H), 2.37–1.48 (m, 4H), 3.04 (dd, 1H, $J_1 = 18.4$ Hz, $J_2 = 3.3$ Hz, pyrazole 4- H_a), 3.38 (dd, 1H, $J_1 = 18.3$ Hz, $J_2 = 11.2$ Hz, pyrazole 4- H_b), 3.48 (s, 2H), 4.63 (t, 1H), 5.68 (dd, 1H, $J_1 = 11.2$ Hz, $J_2 = 3.3$ Hz, pyrazole 5-H), 6.80–6.87 (m, 1H), 6.92–6.95 (m, 1H), 7.00–7.02 (m, 1H), 7.13–7.16 (m, 1H). Anal. calcd for $\text{C}_{17}\text{H}_{22}\text{N}_4\text{O}_4$: C, 58.95; H, 6.40; N, 16.17%. Found: C, 59.20; H, 6.31; N, 15.94%.

4.3. General procedure for the synthesis of compound **7**

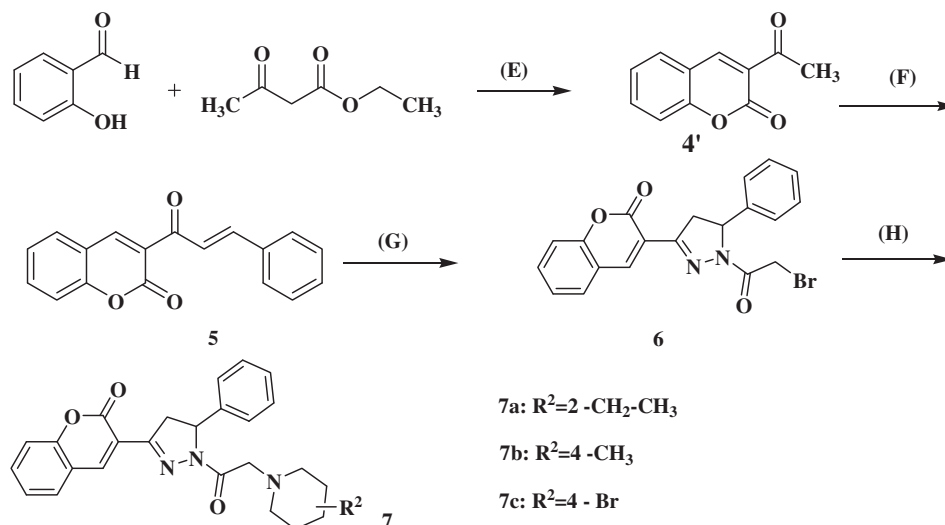
To an acetone (20 mL) solution of 3-(1-(2-bromoacetyl)-5-phenyl-4,5-dihydro-1H-pyrazol-3-yl)-2H-chromen-2-one **6** (10 mmol) was added substituted-piperazine (10 mmol), DMAP (10 mmol) and catalytic KI, the reaction mixture was reflux for 6 h. The mixture was cooled, washed with water. The product was collected by filtration and the crude residue was purified by chromatography on SiO_2 (dichloromethane/methanol, v:v = 70:1) to give title compounds **7a–7c** (Scheme 2) as colorless solids.

4.3.1. 3-(1-(2-(2-Ethylpiperidin-1-yl)acetyl)-3-phenyl-4,5-dihydro-1H-pyrazol-5-yl)-2H-chromen-2-one (**7a**)

Colorless crystals, yield, 60%; mp 210–211 °C; ^1H NMR (400 MHz, CDCl_3) δ (ppm): 0.98 (t, 3H), 1.43 (m, 2H), 1.50–1.69 (m, 6H), 2.06–2.16 (m, 1H), 2.72–2.77 (m, 2H), 3.34 (dd, 1H, $J_1 = 19.2$ Hz, $J_2 = 4.8$ Hz, pyrazole 4- H_a), 3.49 (s, 2H), 3.88 (dd, 1H, $J_1 = 19.2$ Hz, $J_2 = 12.0$ Hz, pyrazole 4- H_b), 5.57 (dd, 1H, $J_1 = 12.0$ Hz, $J_2 = 4.8$ Hz, pyrazole 5-H), 7.19–7.38 (m, 7H), 7.59–7.75 (m, 1H), 7.76–7.78 (m, 1H), 8.67 (1H, s, C₄-H); ^{13}C NMR (CDCl_3 , 125 MHz): δ 9.9, 22.7, 24.0, 28.3, 44.5, 54.2, 61.0, 61.1, 63.1, 63.2, 116.7, 118.7, 125.3, 125.5, 125.6, 127.7, 129.2, 140.6, 140.7, 142.8, 142.9, 153.7, 154.4, 159.3; Anal. calcd for: $\text{C}_{27}\text{H}_{29}\text{N}_3\text{O}_3$: C, 73.11; H, 6.59; N, 9.47%. Found: C, 73.26; H, 6.77; N, 9.86%.

4.3.2. 3-(1-(2-(4-Methylpiperidin-1-yl)acetyl)-3-phenyl-4,5-dihydro-1H-pyrazol-5-yl)-2H-chromen-2-one (**7b**)

Colorless crystals, yield, 59%; mp 209–211 °C; ^1H NMR (400 MHz, CDCl_3) δ (ppm): 0.94 (d, 3H, $J = 4.8$ Hz), 1.60–1.75 (m, 4H), 3.04–3.11 (m, 3H, containing pyrazole 4- H_a), 3.38 (m, 3H), 3.96 (dd, 1H, $J_1 = 19.2$ Hz, $J_2 = 12.0$ Hz, pyrazole 4- H_b), 4.34 (m, 2H), 5.53 (dd, 1H, $J_1 = 4.8$ Hz, $J_2 = 12.0$ Hz, pyrazole 5-H), 7.19–7.35 (m, 9H), 8.76 (1H, s, C₄-H); ^{13}C NMR (CDCl_3 , 125 MHz): δ 21.2, 28.7, 32.0, 44.6, 53.4, 57.4, 61.1, 116.6, 118.5, 118.8, 125.2, 125.6, 128.2, 129.2, 129.7, 133.5, 140.6, 143.2, 153.7, 154.4, 159.3, 164.7; Anal. calcd for: $\text{C}_{26}\text{H}_{27}\text{N}_3\text{O}_3$: C, 72.71; H, 6.34; N, 9.78%. Found: C, 72.90; H, 6.28; N, 10.05%.



Scheme 2. Synthesis of title compound **7**. Reagent and conditions: (E) piperazine, 20–30 °C, 1 h. (F) benzaldehyde, piperidine, ethanol, reflux, 10 h. (G). NH₂-NH₂·H₂O, C₂H₅OH, BrCH₂COOH, reflux, 2 h. (H) substituted piperidine DMAP, KI, reflux, 6 h.

4.3.3. 3-(1-(2-(4-Bromopiperidin-1-yl)acetyl)-3-phenyl-4,5-dihydro-1H-pyrazol-5-yl)-2H-chromen-2-one (**7c**)

Colorless crystals, yield, 55%; mp 200–202 °C; ¹H NMR (400 MHz, CDCl₃) δ (ppm): 1.97–2.16 (m, 4H), 2.28–2.31 (m, 4H), 3.31 (s, 2H), 3.78 (dd, 1H, J₁ = 19.2 Hz, J₂ = 4.8 Hz, pyrazole 4-H_a), 3.52 (m, 1H), 3.90 (dd, 1H, J₁ = 19.2 Hz, J₂ = 12.0 Hz, pyrazole 4-H_b), 5.65 (dd, 1H, J₁ = 4.8 Hz, J₂ = 12.0 Hz, pyrazole 5-H), 7.11–7.38 (m, 9H), 8.70 (1H, s, C₄-H); Anal. calcd for: C₂₅H₂₄BrN₃O₃: C, 60.74; H, 4.89; N, 8.50%. Found: C, 61.02; H, 5.15; N, 8.67%.

4.4. Crystallographic studies

X-ray single-crystal diffraction data for compounds **4d**, **7b** were collected on a Bruker SMART APEX CCD diffractometer at 296(2) K using MoK α radiation (λ = 0.71073 Å) by the ω scan mode. The program SAINT was used for integration of the diffraction profiles. The structures were solved by direct methods using the SHELXS program of the SHELXTL package and refined by full-matrix least-squares methods with SHELXL [14]. All non-hydrogen atoms of compounds **4d**, **7b** were refined with anisotropic thermal parameters. All hydrogen atoms were generated theoretically onto the parent atoms and refined isotropically with fixed thermal factors.

4.5. Anticancer assay

The cytotoxicity evaluation was conducted by using a modified procedure as described in the literature. Briefly, target tumor cells were grown to log phase in RPMI 1640 medium supplemented with 10% fetal bovine serum. After diluting to 3 × 10⁴ cells mL⁻¹ with the complete medium, 100 μ L of the obtained cell suspension was added to each well of 96-well culture plates. The subsequent incubation was performed at 37 °C, 5% CO₂ atmosphere for 24 h before subjecting to cytotoxicity assessment. Tested samples at pre-set concentrations were added to 6 wells with 5-fluorouracil co-assayed as a positive reference. After 48 h exposure period, 25 μ L of PBS containing 2.5 mg mL⁻¹ of MTT was added to each well. After 4 h, the medium was replaced by 150 μ L DMSO to dissolve the purple formazan crystals produced. The absorbance at 570 nm of each well was measured on an ELISA plate reader. The data represented the mean of three experiments in triplicate and were expressed as means \pm SD using Student *t* test. The IC₅₀ value was defined as the concentration at which 50% of the cells could survive.

4.6. Telomerase activity assay

Compounds **4** and **7** were tested in a search for small molecule inhibitors of telomerase activity by using the TRAP-PCR-ELISA assay. In detail, the MGC-803 cells were firstly maintained in DMEM medium (GIBCO, New York, USA) supplemented with 10% fetal bovine serum (GIBCO, New York, USA), streptomycin (0.1 mg/mL) and penicillin (100 IU/mL) at 37 °C in a humidified atmosphere containing 5% CO₂. After trypsinization, 5 × 10⁴ cultured cells in logarithmic growth were seeded into T25 flasks (Corning, New York, USA) and cultured to allow to adherence. The cells were then incubated with Staurosporine (Santa Cruz, Santa Cruz, USA) and the drugs with a series of concentration as 60, 20, 6.67, 2.22, 0.74, 0.25 and 0.0821 g/mL, respectively. After 24 h treatment, the cells were harvested by cell scraper orderly following by washed once with PBS. The cells were lysed in 150 μ L RIPA cell lysis buffer (Santa Cruz, Santa Cruz, USA), and incubated on ice for 30 min. The cellular supernatants were obtained *via* centrifugation at 12,000 g for 20 min at 4 °C and stored at -80 °C. The TRAP-PCR-ELISA assay was performed using a telomerase detection kit (Roche, Basel, Switzerland) according to the manufacturer's protocol. In brief, 2 μ L of cell extracts were mixed with 48 μ L TRAP reaction mixtures. PCR was then initiated at 94 °C, 120 s for predenaturation and performed using 35 cycles each consisting of 94 °C for 30 s, 50 °C for 30 s, 72 °C for 90 s. Then 20 μ L of PCR products were hybridized to a digoxigenin (DIG)-labeled telomeric repeat specific detection probe. And the PCR products were immobilized *via* the biotin-labeled primer to a streptavidin-coated microtiter plate subsequently. The immobilized DNA fragment were detected with a peroxidase-conjugated anti-DIG antibody and visualized following addition of the stop reagent. The microtitre plate was assessed on TECAN Infinite M200 microplate reader (Mannedorf, Switzerland) at a wavelength of 490 nm, and the final value were presented as mean \pm SD.

4.7. General procedure for molecular docking

Discovery Studio 2.1 (DS 2.1, Accelrys Software Inc., San Diego, California, USA). Crystal structure of telomerase (PDB entry 3DU6) was used as template. Hydrogen atoms were added to protein model. The added hydrogen atoms were minimized to have stable energy conformation and to also relax the conformation from close contacts. The active site was defined and sphere of 5 Å was generated around the active site pocket, with the active site pocket of BSAI model using

C-DOCKER, a molecular dynamics (MD) simulated-annealingbased algorithm module from DS 2.1. Random substrate conformations are generated using high-temperature MD. Candidate poses are then created using random rigid-body rotations followed by simulated annealing. The structure of protein, substrate were subjected to energy minimization using CHARMM forcefield as implemented in DS 2.1. A full potential final minimization was then used to refine the substrate poses. Based on C-DOCKER, energy docked conformation of the substrate was retrieved for postdocking analysis.

Acknowledgments

The authors wish to thank the National Natural Science Foundation of China (No.20902003) and the Research fundation of doctor, Anhui Medical University (XJ201120).

References

- [1] W.E. Wright, J.W. Shay, *Curr. Opin. Genet. Dev.* 11 (2001) 98–103.
- [2] A.G. Bodnar, M. Ouellette, M. Frolkis, S.E. Holt, C.P. Chiu, G.B. Morin, C.B. Harley, J.W. Shay, S. Lichtsteiner, W.E. Wright, *Science* 279 (1998) 349–352.
- [3] J.G. Andrew, P.S. Anthony, S. Emmanuel, *Nature* 455 (2008) 633–636.
- [4] F. Hayat, A. Salahuddin, S. Umar, A. Azam, *Eur. J. Med. Chem.* 45 (2010) 4669–4675.
- [5] K.S. Girisha, B. Kalluraya, N. Vijaya, *Eur. J. Med. Chem.* 45 (2010) 4640–4644.
- [6] X.H. Liu, B.F. Ruan, J. Li, B.A. Song, H.L. Zhu, P.S. Bhadury, J. Zhao, *Mini-Rev. Med. Chem.* 11 (2011) 771–821.
- [7] M.L. Neuhouser, *Nutr. Cancer* 50 (2004) 1–7.
- [8] L.W. Min, *Cancer Treat. Rev.* 35 (2009) 57–68.
- [9] X.H. Liu, B.F. Ruan, J.X. Liu, B.A. Song, L.H. Jing, J. Li, Y. Yang, H.L. Zhu, X.B. Qi, *Bioorg. Med. Chem. Lett.* 21 (2011) 2916–2920.
- [10] X.H. Liu, H.F. Liu, J. Chen, Y. Yang, B.A. Song, L.S. Bai, J.X. Liu, H.L. Zhu, X.B. Qi, *Bioorg. Med. Chem. Lett.* 20 (2010) 5705–5708.
- [11] E. Pascolo, C. Wenz, J. Lingner, N. Huel, H. Pripke, I. Kauffmann, P. Garin-Chesa, W.J. Rettig, K. Damm, A. Schnapp, *J. Biol. Chem.* 277 (2002) 15566–15572.
- [12] Y. Peng, I.S. Mian, N.F. Lue, *Mol. Cell* 7 (2001) 1201–1211.
- [13] X.H. Liu, J. Li, F.R. Wu, B.A. Song, P.S. Bhadury, L. Shi, *Med. Chem.* 7 (2011) 605–610.
- [14] G.M. Sheldrick, SHELXL-97, Program for Crystal Structure Solution and Refinement, University of Göttingen, Göttingen, Germany, 1997.